COLD SPRING HARBOR
Molecular Case Studies

RESEARCH ARTICLE

Comprehensive molecular characterization of a rare case of Philadelphia chromosome–positive acute myeloid leukemia

Mara W. Rosenberg,[1,2] Samantha L. Savage,[1,2] Christopher A. Eide,[1,2] Anna Reister Schultz,[1,2] Rachel J. Cook,[2] Richard D. Press,[1,3] Carole Rempfer,[1,3] Garrett Eickelberg,[1,3] Beth Wilmot,[1,4] Shannon K. McWeeney,[1,4] Jeffrey W. Tyner,[1,5] Brian J. Druker,[1,2] and Cristina E. Tognon[1,2]

[1]Knight Cancer Institute, [2]Division of Hematology and Medical Oncology, [3]Department of Pathology, [4]Division of Bioinformatics and Computational Biology, [5]Department of Cell, Developmental, and Cancer Biology, Oregon Health and Science University, Portland, Oregon 97215, USA

Abstract The Philadelphia chromosome (Ph) resulting from the t(9;22) translocation generates the oncogenic BCR::ABL1 fusion protein that is most commonly associated with chronic myeloid leukemia (CML) and Ph-positive (Ph+) acute lymphoblastic leukemia (ALL). There are also rare instances of patients (≤1%) with newly diagnosed acute myeloid leukemia (AML) that harbor this translocation (Paietta et al., *Leukemia* **12:** 1881 [1998]; Keung et al., *Leuk Res* **28:** 579 [2004]; Soupir et al., *Am J Clin Pathol* **127:** 642 [2007]). AML with BCR::ABL has only recently been provisionally classified by the World Health Organization as a diagnostically distinct subtype of AML. Discernment from the extremely close differential diagnosis of myeloid blast crisis CML is challenging, largely relying on medical history rather than clinical characteristics (Arber et al., *Blood* **127:** 2391 [2016]). To gain insight into the genomic features underlying the evolution of AML with BCR::ABL, we identified a patient presenting with a high-risk myelodysplastic syndrome that acquired a BCR::ABL alteration after a peripheral blood stem cell transplant. Serial samples were collected and analyzed using whole-exome sequencing, RNA-seq, and ex vivo functional drug screens. Persistent subclones were identified, both at diagnosis and at relapse, including an *SF3B1*p.Lys700Glu mutation that later cooccurred with an *NRAS*p.Gly12Cys mutation. Functional ex vivo drug screening performed on primary patient cells suggested that combination therapies of ABL1 with RAS or PI3K pathway inhibitors could have augmented the patient's response throughout the course of disease. Together, our findings argue for the importance of genomic profiling and the potential value of ABL1 inhibitor–inclusive combination treatment strategies in patients with this rare disease.

[Supplemental material is available for this article.]

Corresponding author: tognon@ohsu.edu

Ontology terms: acute myeloid leukemia; leukemia

Published by Cold Spring Harbor Laboratory Press

doi:10.1101/mcs.a006218

INTRODUCTION

Philadelphia chromosome-positive acute myeloid leukemia (Ph+ AML) is a rare disease that is not well-understood nor does it present with clearly defined clinical characteristics. There is debate as to whether these patients represent the onset of a true acute leukemia or whether they harbor an asymptomatic chronic phase of chronic myeloid leukemia (CML) until

presenting with progression to myeloid blast crisis (CML–MBC) at diagnosis (Cuneo et al. 1996; Paietta et al. 1998). Previous studies on a limited number of Ph+ AML cases have suggested a few clinical criteria that may distinguish these patients from CML–MBC, including frequent expression of lymphoid markers, no evidence of chronic phase or accelerated phase CML after induction chemotherapy, and a lack of clinical features of CML, such as splenomegaly and basophilia (Tien et al. 1992; Cuneo et al. 1996; Paietta et al. 1998; Ilaria 2005; Soupir et al. 2007; Reboursiere et al. 2015).

BCR::ABL1-positive CML represents a distinct entity within the World Health Organization (WHO) 2016 recommended update to hematologic malignancy diagnostic categories (Arber et al. 2016) and requires identification of the t(9;22) rearrangement by karyotype or cytogenetics and/or detection of the *BCR::ABL1* gene fusion by reverse transcription polymerase chain reaction (RT-PCR). Other diagnoses that clinically resemble CML, but lack BCR::ABL1, include chronic neutrophilic leukemia (CNL); atypical CML; unclassifiable myeloproliferative neoplasm (MPN-U); and unclassifiable myelodysplastic syndrome (MDS)/MPN (MDS/MPN-U). These diagnoses have been shown to coincide with mutation of signaling pathways (e.g., *CSF3R, RAS, CBL*), splicing (e.g., *SRSF2, U2AF1*), or epigenetic regulatory (e.g., *ASXL1, TET2*) genes (Haferlach et al. 2014; Deininger et al. 2017; Zhang et al. 2019).

The presence of *BCR::ABL1* also defines a diagnostic subset of patients with acute lymphoblastic leukemia (ALL). Ph+ ALL is seen in ~20%–30% of adult ALL cases and 3%–5% of pediatric cases (Schlieben et al. 1996; Hunger and Mullighan 2015; Komorowski et al. 2020). Whereas in CML nearly all patients present with the p210 kDa breakpoint isoform of *BCR::ABL1*, patients with Ph+ ALL demonstrate either the p210 isoform or harbor a shorter p190 kDa isoform (~50% each), which retains the identical *ABL1* sequence but lacks the DBL-like and pleckstrin homology domains of BCR (Kurzrock et al. 1988; Faderl et al. 1999; Keung et al. 2004). The p190 isoform is more likely seen in Ph+ B-ALL (~70% of cases) versus Ph+ T-ALL where it is exceedingly rare (Komorowski et al. 2020). Both the p190 and p210 isoforms have been reported to date among molecular studies of Ph+ AML (Piedimonte et al. 2019).

Previous studies have reported cases of the Ph+ clone arising following treatment for a preexisting MDS or AML lacking t(9;22), suggesting some cases may represent a therapy-related AML (Paietta et al. 1998; Onozawa et al. 2003; Keung et al. 2004). Classified as AML with myelodysplasia-related changes by 2016 WHO criteria and AML with t(99;22)(q34.1;q11.2)/BCR::ABL by 2022 European LeukemiaNet (ELN) recommendations, this disease subset has been associated with poor outcomes (Döhner et al. 2022). Here, we describe an in-depth clinical, genetic, and functional screening of a patient with AML with BCR::ABL to improve understanding of the unique molecular pathways contributing to malignant growth and to identify novel effective drug combinations.

RESULTS

Clinical Presentation and Treatment

A 70-yr-old gentleman, previously in good health, was diagnosed with MDS post–presentation of an episode of kidney stones. At diagnosis he had a slightly hypocellular marrow for age (10%–20%) with increased blasts (9% by aspirate counts; 10%–20% by CD34 immunohistochemistry) (Table 1; Supplemental Table 1). The patient was treated with seven cycles of azacytidine. Repeat Marrow studies after cycle four showed a hypocellular marrow (~20%) with trilineage dysplasia and <5% blasts. He underwent a 7/8 DRB1 mismatched unrelated male donor peripheral bone marrow stem cell transplant at 10 mo post–original MDS diagnosis (Fig. 1; thick gray bars), with early post-transplant course uncomplicated and without development of acute or chronic graft-versus-host disease.

Table 1. Clinical and treatment status summary

Specimen ID	Months from initial diagnosis	Disease status	Karyotype	BCR::ABL1 transcripts (%)	Treatment status	Genetrails AML/MDS panel sequencing results
D1.1	0	MDS	45,X,-Y[4]/46,XY[16]	N/A	Azacytidine, well-tolerated	*SF3B1*p.Lys700Glu 13%, *KRAS*p.Gly12Val 11%, *IKZF1*p.Cys492Gly 9%
D1.3	4.7	MDS	46,XY[14]	N/A	Azacytidine; FluMel-conditioned mismatched unrelated donor PBSC transplant	*SF3B1* 7%, *KRAS* 4%, *IKZF1* 4%
RM1.2	9.3	MDS	46,XY[19]	N/A	Day +32, no evidence of disease by peripheral smear	No mutations
R1.1	15.7	Ph+ AML	45,X,-Y,t(9;22)(q34;q11.2)[3]/46,XY[17]	N/A	BCR::ABL1 detected	Low-level *SF3B1*, no other mutations
R1.2	16.3	Ph+ AML	45,X,-Y,t(9;22)(q34;q11.2)[14]/49,sl,+19,+21, +der(22)t(9;22)(q34;q11.2),+mar[6]/46,XY[3]	113.8%	Started azacytidine + dasatinib	Low-level *SF3B1* and *NRAS*p.Gly12Cys; no other mutations
R1.3	17.0	Ph+ AML	45,X,-Y,t(9;22)(q34;q11.2)[3]/46,XY[20]	11.5%	Azacytidine + dasatinib	Not tested
RM2.1	20.7	Ph+ AML	46,XY[17]	Undetected	Azacytidine + reduced dose dasatinib, toxicity	No mutations
RM2.2	22.7	Ph+ AML	46,XY[17]	Undetected	Azacytidine + reduced dose dasatinib	No mutations
RM2.4	28.1	Ph+ AML	Not tested	0.017%	Short cycle of nilotinib + azacytidine due to dasatinib toxicity	No mutations
RM2.5	34.4	Ph+ AML	49,X,-Y,t(9;22)(q34;q11.2), + 19,+21,+der(22)t (9;22),+mar[5]/46,XY[15]	1.6%	Started ponatinib + azacytidine	No mutations detected w/ Genetrails (ABL1 kinase domain sequencing detected *ABL1*p.Gln252His 20%)
RM2.6	37.0	Ph+ AML	46,XY[20]	0.56%	Ponatinib + azacytidine	No mutations
R2.1	40.2	Ph+ AML	48~49,X,-Y,add(3)(q21),t(3;12)(q25;q24.1), add (8)(q22),t(9;22)(q34;q11.2),+19,+21,+der(22)t (9;22)(q34;q11.2),+mar[cp7]/48~50,+12,-der (12)t(3;12)(q25;q24.1)[cp12]/46,XY[1]	72%	Begin FLAG/Ida	*NRAS* 17%, *SF3B1* 21%
R2.4	41.4	Ph+ AML	49,X,-Y,add(3)(q21),t(3;12), (q25;q24.1),add(8) (q22),t(9;22)(q34;q11.2),+19,+21,+der(22)t (9;22)(q34;q11.2),+mar[2]/48~49,idem,+12, der(12)t(3;12)(q25;q24.1)[cp12]/46,XY[6]	19%	Day 39 FLAG/Ida	*NRAS* 1%, *SF3B1* 1%
R2.5	43.2	Ph+ AML	Not tested	84%	10 d course of decitabine, DLI infusion, Started bosutinib + decitabine	Not tested

Specimen ID corresponds to disease stage: (D) diagnosis, (RM) remission, (R) relapse, (first number) instance of stage, (second number) samples number. For example, (RM2.5) is the fifth sample taken during the second remission. Sample dates have been adjusted to months since the patient's initial diagnosis to maintain confidentiality.
(AML) Acute myeloid leukemia, (MDS) myelodysplastic syndrome, (N/A) not available, (PBSC) peripheral blood stem call, (Ph+) Philadelphia chromosome–positive.

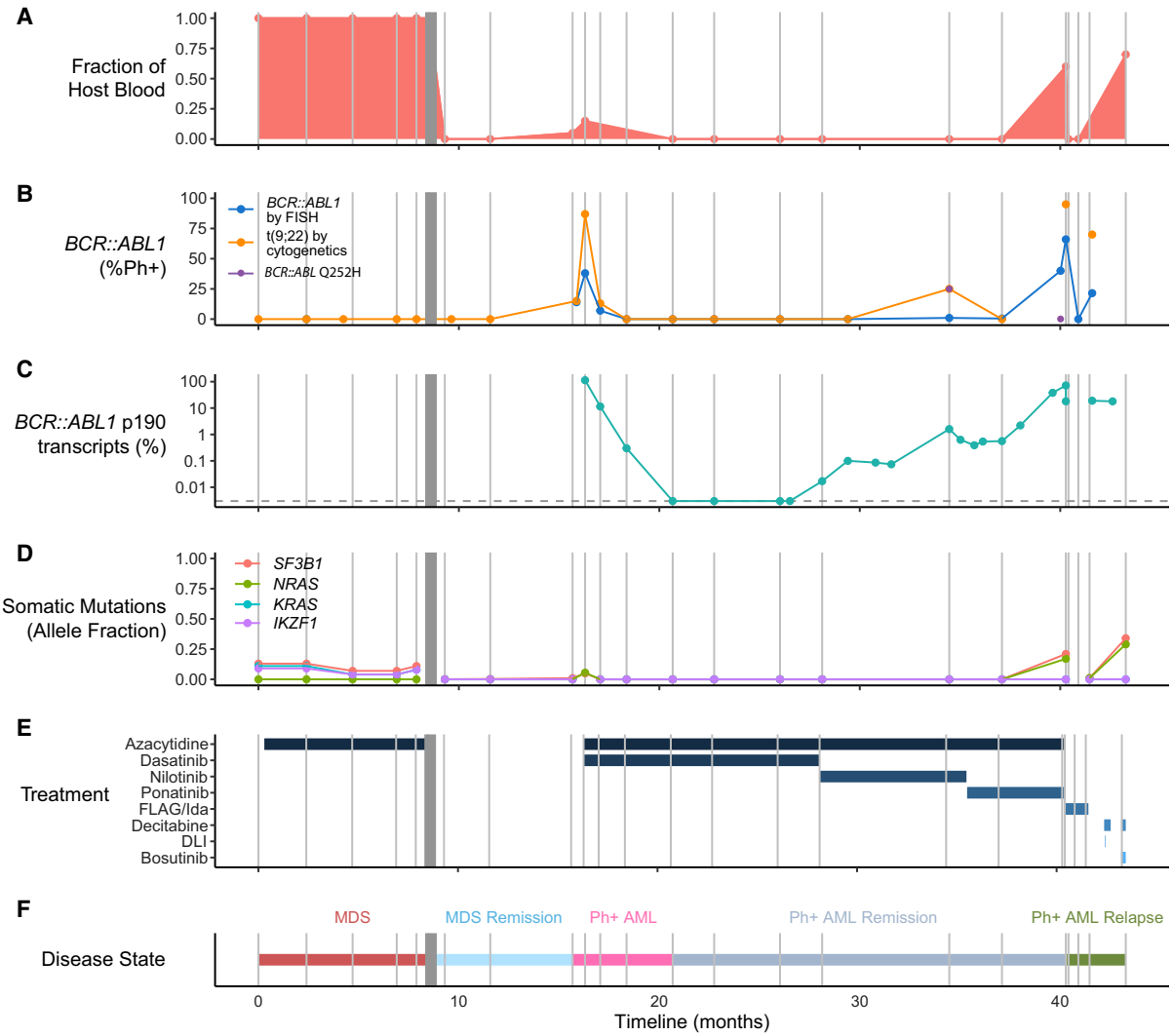

Figure 1. Longitudinal genomic profiling of a patient transformed from myelodysplastic syndrome (MDS) to acute myeloid leukemia (AML) with BCR::ABL. (*A*) Fraction of blood in the circulation attributed to host versus stem cell transplant donor. (*B*) *BCR::ABL1* percentage positivity (% Ph+) as assessed by fluorescence in situ hybridization (FISH) (blue) or t(9;22) cytogenetics (orange). (*C*) *BCR::ABL1* p190 fusion transcript levels, normalized and reported as the percentage relative to expressed *ABL1* transcripts (log scale). (*D*) Somatic driver point mutations as identified by a clinical deep sequencing panel (GeneTrails; see Methods). (*E*) Treatment time line for the course of disease. (DLI) donor lymphocyte infusion. (*F*) Clinical diagnosis throughout disease course with disease status at each time point. (Thick gray bar) Mismatched unrelated donor peripheral blood stem cell transplant time point. (Thin gray bars) Time points with whole-exome sequencing, RNA sequencing, or targeted sequencing.

The patient was noted seven months post-transplant to have myeloid blasts in his peripheral blood smear, leading to a repeat bone marrow biopsy, which showed increased myeloid blasts (~5%). Fluorescence in situ hybridization (FISH) was 14% positive for the *BCR::ABL1* fusion. *BCR::ABL1* p190 transcript levels increased with increasing host cell burden (Fig. 1A,B), consistent with the *BCR::ABL1*-positive clone arising from residual host cells (Fig. 1C). At this time, he was treated with the ABL1 tyrosine kinase inhibitor (TKI) dasatinib

in addition to azacytidine. Repeat marrow studies after one cycle showed an ~10-fold reduction in *BCR::ABL1* transcripts, a hypocellular marrow (~20%) with erythroid predominant trilineage hematopoiesis, and ~5%–10% myeloid blasts. He continued on this regimen for an additional 9 mo, at which point previously identified mutations were undetectable, FISH studies were negative for *BCR::ABL1*, and *BCR::ABL1* transcript levels were only weakly positive.

Because of treatment-related toxicities from dasatinib that persisted despite dose reductions, treatment was changed to nilotinib (150 mg BID). However, after 8 mo, evidence of molecular relapse was observed with respect to *BCR::ABL1* transcripts, tracking with the emergence of an *ABL1*p.Gln252His (20%) mutation in the kinase domain of *BCR::ABL1*, known to be associated with moderate resistance to nilotinib (O'Hare et al. 2005; McCarron et al. 2013). As a result, the patient was switched to ponatinib (15 mg QD) (Fig. 1E).

Five months after initiation of ponatinib, repeat marrow studies revealed a hypercellular marrow with severe myelofibrosis and increased blasts (58%) as well as a complex karyotype. Subsequent short courses of decitabine with donor lymphocyte infusion (DLI) and bosutinib (200 mg QD) were provided without effect, and 4 d later the patient succumbed to his disease.

Genomic Analysis

To understand the full evolution of this patient's disease, we first analyzed the pattern of somatic mutations acquired throughout treatment. Mutations were determined with a CLIA-certified clinical targeted next-generation sequencing (NGS) panel of 42 genes, validated at Oregon Health and Science University (OHSU) as part of standard clinical practice. Exome sequencing on tumor samples was also performed from nine time points with available stored material, spanning the full course of disease and treatment.

The patient presented with *SF3B1*p.Lys700Glu, *IKZF1*p.Cys492Gly, and *KRAS*p.Gly12Val variants detected at variant allele frequency (VAF) levels of 13%, 9%, and 11%, respectively (GeneTrails, with similar VAF levels noted in corresponding whole-exome sequencing [WES] data; Table 2; Supplemental Table 2). The patient had no detectable *BCR::ABL1* fusion upon initial diagnosis of MDS. At the time of post-transplant progression outgrowth of a newly detected *BCR::ABL1* fusion, a new *NRAS*p.Gly12Cys mutation (5%) and return of the *SF3B1*p.Lys700Glu (5%) original founder clone were observed (Table 2; Fig. 1B–D). The addition of dasatinib and later nilotinib therapies to azacytidine led to a deep molecular response, with relapse at least partly attributable to acquisition of a Q252H nilotinib-resistant mutation in the *BCR::ABL1* kinase domain. Although at this time point none of the previous driver mutations, outside of *BCR::ABL1*, were detected, subsequent relapse on ponatinib showed *BCR::ABL1* transcripts at near Ph+ AML diagnosis levels, along with a new *NRAS*p.Gly12Cys mutation and the previously observed *SF3B1*p.Lys700Glu at similar VAF (17% and 20%, respectively; Table 2; Fig. 1D; Supplemental

Table 2. High-confidence somatic mutations identified in patient samples

Gene	Chromosome	HGVS DNA reference	HGVS protein reference	Variant type	Predicted effect	dbSNP/ dbVar ID	Genotype	Exome coverage
SF3B1	Chr 2:198266834	T > C	p.K700E	Missense	Deleterious	NA	Somatic	130×–230×
NRAS	Chr 1:115258748	C > A	p.G12C	Missense	Deleterious	NA	Somatic	130×–230×
KRAS	Chr 12:25398284	C > A	p.G12V	Missense	Deleterious	NA	Somatic	130×–230×
IKZF1	Chr 7:50468239	T > G	p.C492G	Missense	Deleterious	NA	Somatic	100×–150×

Table 2). At this relapsed time point, the *BCR::ABL1p.Gln252His* mutation was no longer detectable, consistent with ponatinib's potent efficacy against this variant. Together, these findings suggest the patient exhibited an original *SF3B1* mutant founder clone, a *KRAS* and *IKZF1*-mutated subclone of which was eliminated with azacytidine and transplant, with subsequent expansion of a new *BCR::ABL1*-positive subclone upon transformation to AML with BCR::ABL. This subclone responded to azacytidine + ABL1 TKI treatment, but an additional *NRAS* mutation, which could have arisen in this clone or a separate subclone, was selected for at the time of ponatinib resistance.

FLAG-Ida (fludarabine, cytarabine, granulocyte colony-stimulating factor [G-CSF], idarubicin) treatment temporarily reduced the ponatinib-resistant disease to undetectable levels, but the patient ultimately relapsed. Within the relapsed sample, *BCR::ABL1* transcripts were at 72% by PCR and the same *SF3B1pLys700Glu* mutation from the initial sample was present at 21%. New mutations in *NRAS* (17%), and cytogenetic changes in *RUNX1* (63%), *NUP214* (65%), and *MECOM* (63%) were also identified using NGS and FISH, respectively (Table 2; Fig. 1D–F). Of note, there was no confirmed evidence of the *DEK::NUP14* and *MECOM::RPN1* fusion directly, only of increased expression of *NUP14* and *MECOM* suggestive of a fusion. This final FLAG-Ida-relapsed sample also contained an outgrowth of the host cells (identified and tracked through germline mutations) in addition to revealing 109 newly identified mutations not seen in previous samples (Supplemental Table 5), including *GATA2*p.Ala318Thr, a known gain-of-function mutation with myelopoiesis-stimulating activity in AML (Katsumura et al. 2018). It is likely that many of these other acquired mutations are passenger events secondary to FLAG-Ida regimen, the full significance of which is difficult to determine from this single case study (Fig. 2A; Patel et al. 2012).

To complement the findings of mutation clonality and selection, RNA sequencing (RNA-seq) was performed at seven different time points throughout the course of this patient's disease (Fig. 2B; Supplemental Tables 3 and 6). Samples were classified as either low disease burden (<10% blast count; $N = 4$; cluster group blue) or high disease burden (>20%, $N = 2$; cluster group green) with the latter two sequenced during the final post-ponatinib and post-FLAG-Ida treatment relapses. Differential gene expression analysis identified 25 genes with significantly increased expression in the high disease burden, relapsed samples compared with the low disease burden, prerelapse specimens (Fig. 2B; see Methods and Supplemental Table 3), including *ABL1*, consistent with increased levels of *BCR::ABL1*-positive disease. We also noted overexpression of *NPM1* in the Ph+ relapse samples. Although mutations in this gene are observed in ~30% of AML patients (Sportoletti 2011) and rare cases of AML harboring *NPM1* mutations along with *BCR::ABL1* have been described previously (Neuendorff et al. 2016; Catalano et al. 2020), no mutations in *NPM1* were detected at the time of relapse in this patient. Other notable overexpressed genes included *EEF2* and *IRAK1BP1*. Higher expression of *EEF2* has been observed in multiple solid and hematologic cancer types (Nakamura et al. 2009; Oji et al. 2014). IRAKBP1 has been shown to be phosphorylated by IRAK1 (interleukin-1 receptor-associated kinase) (Conner et al. 2010). *IRAK1* has been observed to be overexpressed in 20%–30% of MDS patients, and overexpression in AML patients has been shown to provide a survival signal, which can be targeted with small-molecule inhibitors such as pacritinib (Hosseini et al. 2018).

Functional Analysis

We performed an ex vivo drug sensitivity screen with a panel of clinically relevant small-molecule inhibitors as previously described (Tyner et al. 2013; Tyner et al. 2018) on two specimens (R2.1 and R2.5) that were obtained from the patient when the disease burden was the highest. Specimen R2.1 was obtained at month 40.2 while the patient was on Flag/Ida and possessed

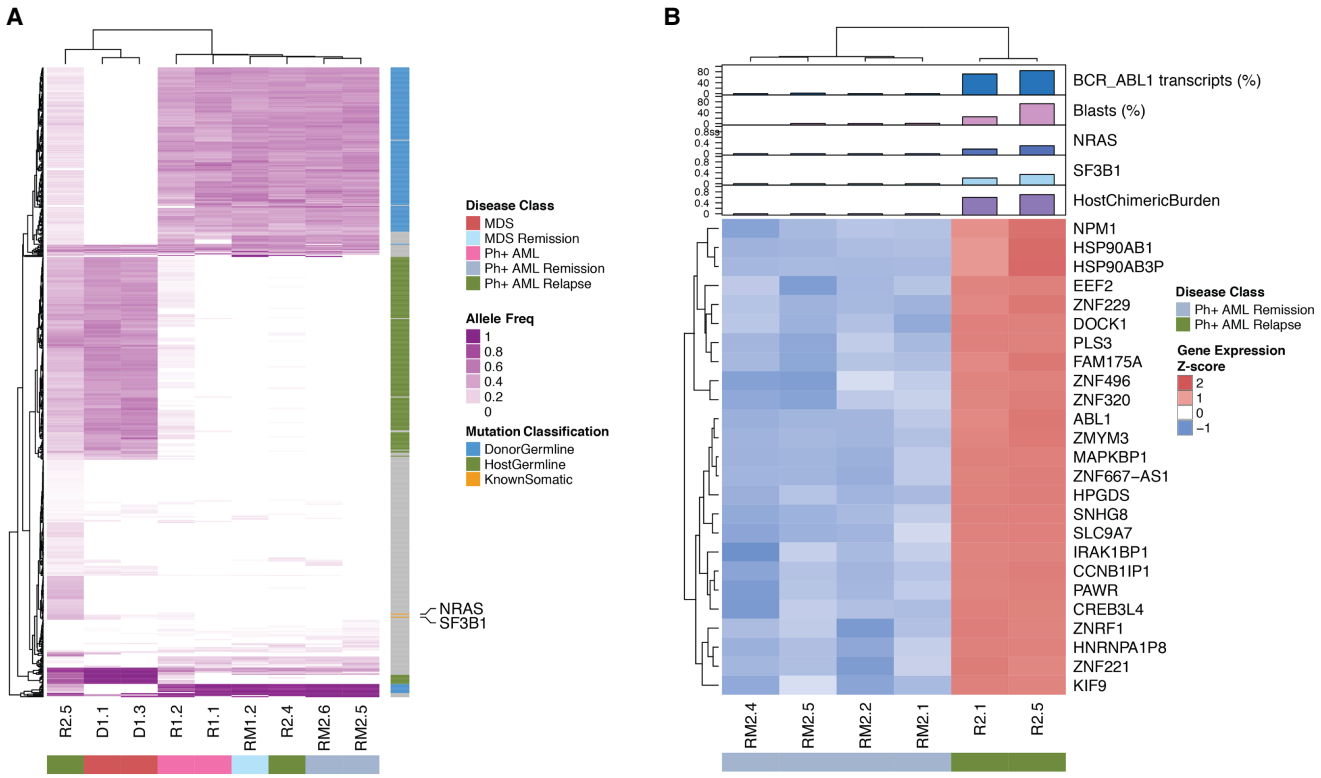

Figure 2. Whole-exome sequencing and RNA sequencing gene expression profiling identifies distinct clusters of samples demonstrating unique characteristics throughout the disease course. (*A*) Hierarchical clustering performed on the Euclidean distance between allele frequency of mutations identified at the last relapse time point. Mutations were excluded if present at >0.4 allele fraction pre-bone marrow transplant (BMT) and the two remission time points immediately post-BMT. This removes common variants in both the host and donor. Donor (blue) and host germline (green) mutations were identified as those at ≥0.3 allele fraction in pre-BMT and immediately post-BMT, respectively, outside the 95% confidence interval (CI) of expected driver somatic events. Three clusters of mutations are observed: those comprised dominantly of host germline events, donor germline events, and the last relapse sample displaying a mix between both host and donor along with unique somatic mutations not previously identified. Known somatic mutations in *NRAS* and *SF3B1* are highlighted in yellow. (*B*) Differential gene expression comparing Philadelphia chromosome–positive (Ph+) remission (blue cluster) and relapsed, resistant samples (green cluster). Scaled expression values are shown as *z*-scores in the heatmap, with annotations of *BCR::ABL1* transcripts, blast percentage, mutation variant allele frequency (VAF), and host/donor chimerism percentage indicated above.

72% *BCR::ABL* transcripts. Specimen R2.5 was obtained at month 43.2, 1 d after the patient was provided decitabine/bosutinib and possessed 84% *BCR::ABL* transcripts.

Specimen R2.5 exhibited increased sensitivity to dasatinib compared to Specimen R2.1 (Fig. 3A; select TKIs plotted; select drug targets described in Supplemental Table 4), consistent with the outgrowth of the *BCR::ABL1*-positive clone and the patient's initial response to dasatinib before subsequent discontinuation due to drug toxicity. Increased sensitivity to ponatinib, nilotinib, sunitinib, and sorafenib was also observed. Focusing on the final relapse time point, we also assessed this patient's ex vivo drug response profile compared to the response of all patient samples screened to date at our institution for those given drugs. The patient's tumor sample ranked among the most sensitive (lowest 10%) of all samples tested with a given drug by area under the curve (AUC) for select ABL1 (dasatinib; PD173955), PI3K/mTOR (PHT-427; rapamycin), and MAPK (trametinib) inhibitors (Fig. 3B; blue with AUC

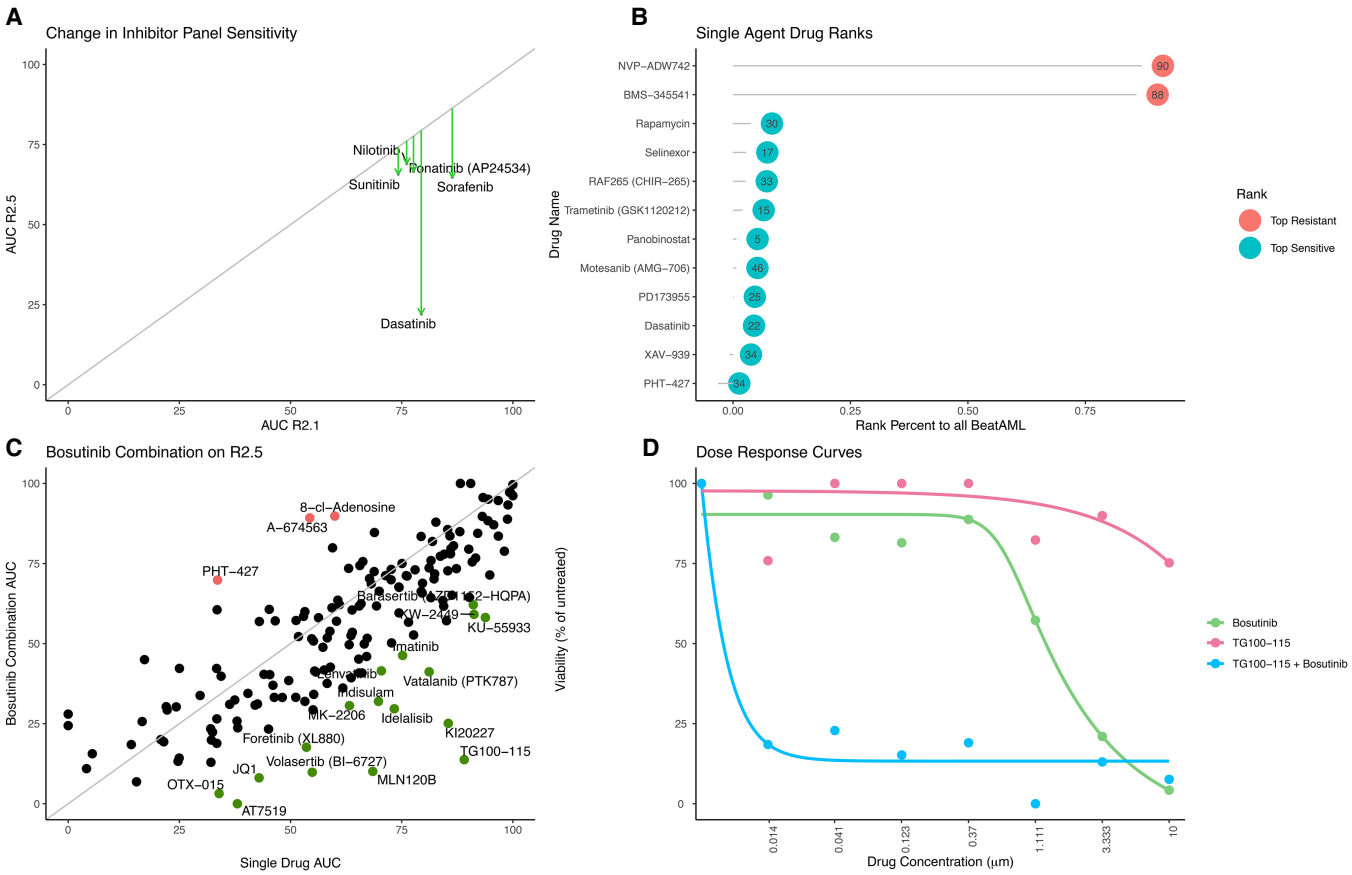

Figure 3. Ex vivo profiling of relapsed acute myeloid leukemia (AML) with BCR::ABL sample reveals sensitivity to select small-molecule inhibitors alone and in combination. (*A*) Change in inhibitor sensitivity profile (as measured by the area under the curve [AUC]) between relapse (R2.1 and R2.5) specimens. Five select drugs, all indicated on the plot, demonstrated variable degrees of increased sensitivity in the final R2.5 sample (as shown by the magnitude of the green arrows). (*B*) Comparison of the drug sensitivity profile for this patient at the R2.5 time point with AUC values from all historically collected leukemia samples tested with the same inhibitors (n = 1831). Labeled drugs are those where the patient AUC was in the top (insensitive; red) or bottom (sensitive; teal) 10% of AUC values across all samples. Numbers inside circles represent the percentage of the median AUC for the given drug. The median AUC is calculated across all samples ever tested with a given drug. Drugs are considered particularly sensitive in a patient sample if they are <20% of the median AUC (Tyner et al. 2013). (*C*) Comparison of AUC values for inhibitors alone versus upon combination with 50 nM bosutinib in relapse sample R2.5. Green and red highlights indicate drugs with greater than twofold AUC decrease or increase, respectively. (*D*) Individual drug sensitivity curves for bosutinib (green) and PI3K inhibitor TG100-115 (red) alone and in combination (blue).

values listed within the circle). Notably, the trametinib sensitivity was consistent with the observed acquisition of an *NRAS* mutation at relapse (Fig. 1C).

Next, we sought to identify drugs that could be used in combination with the ABL1 TKI bosutinib, which was provided to the patient 1 d prior to final sample collection. The patient was only on this drug for a brief period; therefore, clinical response could not be determined. However, the ex vivo screen provides a window into combinations that may allow improved response for future patients. Similar drug sensitivity ex vivo screens were performed with an overlay concentration of 50 nM bosutinib (a concentration sufficient to inhibit BCR::ABL1 kinase activity in the drug assay) in every well. We observed increased bosutinib sensitivity

when combined with several drugs, including the PI3K inhibitors TG100-115 and idelalisib or the ATM inhibitor KU-55933 (Fig. 3C,D). These findings underscore the potential utility of combination therapies to target tumor pathways activated by multiple mutations.

DISCUSSION

Our results contribute to the understanding of the rare AML with BCR::ABL subtype of acute myeloid leukemia and represent the first study to characterize this disease with extensive longitudinal genomic data as well as ex vivo small-molecule inhibitor screens. In this case study, we follow the disease evolution from initial presentation with MDS through post-transplant, relapsed disease transforming to AML harboring a t(9;22) translocation and p190 *BCR::ABL1* isoform as the new driver mutation.

By differential gene expression analysis, we noted overexpression of *NPM1*, *EEF2*, and *IRAKBP1* in the Ph+ samples. Although mutations in *NPM1* are observed in ~30% of AML patients (Sportoletti 2011) and rare cases of AML harboring *NPM1* mutations with BCR::ABL1 have been described previously (Neuendorff et al. 2016; Catalano et al. 2020), no mutations in *NPM1* were detected at the time of relapse in this patient. Other notable overexpressed genes included *EEF2* and *IRAK1BP1*. Higher expression of *EEF2* has been observed in multiple solid and hematologic cancer types (Nakamura et al. 2009; Oji et al. 2014). IRAKBP1 has been shown to be phosphorylated by IRAK1 (Conner et al. 2010). *IRAK1* has been observed to be overexpressed in 20%–30% of MDS patients, and overexpression in AML patients has been shown to provide a survival signal that can be targeted with small-molecule inhibitors such as pacritinib (Hosseini et al. 2018).

Further, ML has been defined by its heterogeneity with respect to presentation and clinical outcome, and nearly 50% of AML patients have a normal karyotype (Patel et al. 2012; Cancer Genome Atlas Research Network et al. 2013). A small percentage (1.5%) (Cancer Genome Atlas Research Network et al. 2013) of AML patients harbor *BCR::ABL1*, and the WHO recently classified Ph+ AML as diagnostically distinct from myeloid blast crisis CML (Arber et al. 2016). For example, the p190 isoform of *BCR::ABL1* harbored by the patient in this study has been observed in ~50% of Ph+ AML, whereas the p210 isoform is present in nearly all cases of CML, including those with blast crisis (Score et al. 2010).

This case study confirms that ABL1 TKI therapy can be an effective initial treatment for patients with AML with BCR::ABL. However, because of the heterogeneity of disease, resistance is inevitably acquired through diverse mechanisms. In this case study, we observed BCR::ABL1 kinase domain mutation-mediated resistance to nilotinib and later potential BCR::ABL1 kinase-independent resistance via the acquisition of an activating $NRAS^{G12C}$ mutation. Of note, a targetable dependency on RAS signaling has been shown to occur in patients with acquired resistance to ABL1 TKIs in the context of CML (Chu et al. 2004; Agarwal et al. 2008; Packer et al. 2011; Asmussen et al. 2014). Our functional genomic assessment of this patient suggests that it may be possible to overcome these resistance mechanisms by using combinations of ABL1 TKIs with RAS pathway inhibitors such as trametinib or PI3K inhibitors such as TG100-115 or idelalisib. Upfront combination therapy treatment may be needed to circumvent resistance in these hard-to-treat patients.

METHODS

Patient

The patient in this case study was diagnosed and treated at OHSU, and informed consent was obtained under protocol IRB#4422. To maintain confidentiality, all dates have been

adjusted to months since the patient's initial diagnosis. Relative spacings between time points are maintained.

Custom Gene Panel (GeneTrails) Variant Detection

Sequencing of a panel of 42 AML/MDS-associated genes was performed as part of standard clinical care through the CLIA-certified OHSU Knight Diagnostics Laboratory (GeneTrails, CLIA #38D201825). The custom capture panel of 42 genes is a set known to play a role in leukemia pathogenesis, prognosis, or response to therapy and include *ABL1*, *ASXL1*, *BCOR*, *CBL*, *CBLB*, *CEBPA*, *CREBBP*, *CSF3R*, *DNMT3A*, *ETV6*, *EZH2*, *FBXW7*, *FLT3*, *GATA1*, *GATA2*, *HRAS*, *IDH1*, *IDH2*, *IKZF1*, *IL7R*, *JAK1*, *JAK2*, *JAK3*, *KDM6A*, *KIT*, *KRAS*, *MPL*, *NOTCH1*, *NPM1 NRAS*, *PAX5*, *PTPN11*, *RUNX1*, *SF3B1*, *SRSF2*, *STAT3*, *SUZ12*, *TET2*, *TP53*, *U2AF1*, *WT1*, and *ZRSR2*.

Genomic DNA was extracted and purified from blood or bone marrow and sequenced by NGS using multiplexed PCR (AmpliSeq primers) and emulsion PCR, followed by semiconductor-based sequencing on an Ion Torrent PGM. Gene segments that were not easily covered by NGS were covered instead by Sanger dideoxy sequencing methods. The minimum limit of detection for the GeneTrails assay is 5%–15% depending on sequence read depth, with minimum sequence coverage at a depth of 100X.

Whole-Exome Sequencing

An Illumina Nextra RapidCapture probe set and protocol were used, which provided coverage of 37 Mb of genomic DNA coding regions. Sequence methods and variant detection were performed as per protocols of the Beat AML study (Tyner et al. 2018). Average sequence depth across all samples at 500×. Briefly, following initial QC on a TapeStation (Agilent), 50 ng of intact genomic DNA was fragmented and tagged (tagmentation) in a single step. Following cleanup, the tagmented DNA was amplified by 10 cycles of PCR, which added the indexed adaptors for clustering and sequencing. Libraries were hybridized to capture pools in 12 sample sets with two rounds of hybridization performed to increase specificity. Libraries recovered with streptavidin magnetic beads were amplified by 10 cycles of PCR, unincorporated reagents were removed with AMPure beads (Agencourt), and validated on the TapeStation. Quantification of capture pools was done using real time PCR (Kapa). Libraries were denatured, flow cells set up using the cBot (Illumina) and run on an Illumina HiSeq 2500 using paired-end 100-cycle protocols. Five or six lanes were run per capture group.

Whole-Exome Sequencing Data Processing

Initial data processing and alignments were performed with commonly used analytical tools. For each flow cell and each sample, the FASTQ files were aggregated into single files for read 1 and 2. During this process these reads were trimmed by 3 on the 5′ end and 5 on the 3′ end. BWA MEM version 0.7.10-r789 (Li and Durbin 2009) was used to align the read pairs for each sample-lane FASTQ file. As part of this process, the flow cell and lane information was kept as part of the read group of the resulting SAM file. The Genome Analysis Toolkit (v3.3) and the bundled Picard (v1.120.1579) were used (McKenna et al. 2010) for alignment postprocessing. Files contained within the Broad's bundle 2.8 were used, including their version of the build 37 human genome (these files were downloaded from ftp://ftp.broadinstitute.org/bundle/2.8/b37/).

The following steps were performed per sample-lane SAM file generated for each CaptureGroup.

- The SAM files were sorted and converted to BAM via SortSam.

- MarkDuplicates was run, marking both lane level standard and optical duplicates.
- Reads were realigned around indels from the reads–RealignerTargetCreator/IndelRealigner.
- Base Quality Score Recalibration was performed.

The resulting BAM files were then aggregated by sample and an additional round of MarkDuplicates was carried out at the sample level. Quality control reports were generated using the ReportingTools (Huntley et al. 2013) and qrqc Bioconductor R packages along with output files from the sequencing core and the alignment output files. Indel realignment was done at the sample level.

Whole-Exome Sequencing Variant Detection

Each sample with exome sequencing was genotyped for single nucleotide variations using Mutect v.1.1.7 (Cibulskis et al. 2013). As there was no matched normal for this patient, Mutect was run using default parameters. Indels were identified using Varscan2 v 2.4.1 in mpileup2indel mode (Koboldt et al. 2012). Each VCF was annotated using the Variant Effect Predictor v83 against GRCh37 (McLaren et al. 2010). The resulting VCF files were filtered to include only those annotated to a gene and were converted to MAF format using the vcf2maf v1.6.6 tool. Mutations were filtered for common germline variants by excluding mutations seen in >1% population VAF from ExAC database (Lek et al. 2016). Driver events previously identified through the clinical sequencing gene panel were retained.

RNA Sequencing

RNA sequencing was performed using the Agilent SureSelect Strand-Specific RNA Library Preparation Kit. All sequencing was performed on an Illumina HiSeq 2500. All samples were sequenced using the Agilent SureSelect Strand-Specific RNA Library Preparation Kit on the Bravo robot (Agilent). Briefly, poly(A)$^+$ RNA was chemically fragmented. Double stranded cDNAs were synthesized using random hexamer priming with 3′ ends of the cDNA adenylated then indexed adaptors were ligated. Library amplification was performed using three-primer PCR using a uracil DNA glycosylase addition for strandedness. Libraries were validated with the Bioanalyzer (Agilent) and combined to run four samples per lane, with a targeted yield of 200 million clusters. Combined libraries were denatured, clustered with the cBot (Illumina), and sequenced on the HiSeq 2500 using a 100-cycle paired-end protocol.

In addition to the AML samples, there was also a sample of purified CD34$^+$ cells from healthy control bone marrow, which was included in each sample group (for a total of 12 times sequencing this control RNA). This control served as both a healthy comparator and a quality check on intergroup batch effects. Twenty-one additional individual healthy bone marrow samples were also included, two of which were CD34– selected (17-00053 and 17-00056) with the other 19 being whole mononuclear bone marrow cells from healthy donors. For each flow cell and each sample, the FASTQ files were aggregated into single files for read 1 and read 2 (if not already done by the sequencing core). During this process these reads were trimmed by 3 on the 5′ end and 5 on the 3′ end. Alignments of reads were performed using the subjunc aligner (1.5.0-p2) (Liao et al. 2013). BAM files obtained from subjunc were used as inputs into featureCounts (1.5.0-p2) (Liao et al. 2014) and gene-level read counts were produced.

For a reference genome, the GRCh37 build provided by the Broad as part of the GATK bundle was used. Gene assignments were based on the Ensembl build 75 gene models on GRCh37. See the parameters below for software usage: subjunc -i /path/to/reference/ -u -r fastq1 -R fastq2 -o outputBAMFilename -I 5 -T 7 -d 50 -D 600 -S frfeatureCounts -a

Homo_sapiens.GRCh37.75.gtf -o output -F GTF -t exon -g gene_id -s 2 -C -T 10 -p -P -d 50 -D 600 -B BAM_files

Final counts were then used for downstream analyses.

RNA Sequencing Expression Analysis

RNA sequencing analyses were postprocessed using EdgeR v3.7 (McCarthy et al. 2012). Counts per transcript were normalized through conversion to cpm. Transcripts were retained if they had values of >1 cpm in at least two out of the four RNA-seq samples with low blast count and in at least one of the two high blast samples. Those lower than these values were filtered out. The largest expressed transcript was chosen to represent expression for that gene. Differentially expressed genes between low and high blast count sample groups were nominated as those genes that had mean within group coefficient of variance <13.5 and log fold change between the two groups of >2. The low sample number and similarity between samples being from the same patient limited use of common differential expression algorithms.

Ex Vivo Functional Drug Screens

Ex vivo functional drug screens were performed on freshly isolated mononuclear cells from AML samples as previously described (Tyner et al. 2013). Briefly, for each sample, cells were treated with a panel of inhibitors (each in a seven-dose, threefold dilution series [from 10 μM to 0.014 μM]), cultured for 3 d, and assessed for viability using a tetrazolium-based colorimetric assay. Absorbance values (optical density at 490 nm) were blanked and normalized as a percent of the mean of untreated control wells. These normalized viability values were confined to a 0%–100% range to produce a response variable for analysis.

Drug sensitivity was quantified as the area under the fitted seven-point probit curve via direct integration. The fitted probit curve used the discrete drug concentrations as *x*-values and the cell viability with limits 0% to 100% as the *y*-values. AUC values were normalized to the maximum possible AUC value for the tested dose range. Calculations were made for each sample for single drug or drug combination pairings.

ADDITIONAL INFORMATION

Data Deposition and Access

All data from gene sequencing panels is provided in Table 1. Exome variants are found in Supplemental Table 1, and supporting data has been deposited into dbGaP (study ID 30641; accession ID phs001657.v2.p1; subject ID 2801). High confidence somatic mutations are annotated in Table 2 and the variants were submitted to ClinVar (https://www.ncbi.nlm.nih.gov/clinvar/) and can be found under accession numbers SCV002583832–SCV002583835.

Ethics Statement

Written consent was obtained by the patient under IRB protocol #4422 and reviewed by the Institutional Review Board at Oregon Health & Science University.

Acknowledgments

We sincerely thank the patient described in this study and dedicate this work to him. He was an avid reader and always up-to-date on the newest scientific abstracts on his disease. We also thank Dr. Jessica Leonard for her input on *BCR::ABL* p190 molecular monitoring.

Competing Interest Statement

J.W.T. received research support from Agios, Aptose, Array, AstraZeneca, Constellation, Genentech, Gilead, Incyte, Janssen, Petra, Seattle Genetics, Schrodinger, Syros, Takeda, and Tolero. B.J.D. was an Investigator with the Howard Hughes Medical Institute and is supported by the National Institutes of Health/National Cancer Institute (NIH/NCI) (2R01CA065823-21A1) and the Knight Cancer Research Institute. B.J.D. has potential competing interests– SAB: Adela Bio, Aileron Therapeutics, Therapy Architects (ALLCRON), Cepheid, Celgene, RUNX1 Research Program, Nemucore Medical Innovations, Novartis, Vivid Biosciences (inactive), Gilead Sciences (inactive); SAB and stock: Aptose Biosciences, Blueprint Medicines, EnLiven Therapeutics, Iterion Therapeutics, GRAIL, Recludix Pharma; Scientific Founder: MolecularMD (inactive, acquired by ICON); Board of Directors and stock: Amgen, Vincerx Pharma; Board of Directors: Burroughs Wellcome Fund, CureOne; Joint Steering Committee: Beat AML LLS; founder: VB Therapeutics; Sponsored Research Agreement: EnLiven Therapeutics, Recludix Pharma; clinical trial funding: Novartis, Astra-Zeneca; Royalties from Patent 6958335 (Novartis exclusive license) and Oregon Health and Sciences University and Dana-Farber Cancer Institute (one Merck exclusive license, one CytoImage, Inc. exclusive license, and one Sun Pharma Advanced Research Company nonexclusive license); U.S. Patents 4326534, 6958335, 7416873, 7592142, 10473667, 10664967, 11049247. C.E.T. received research support from Ignyta (inactive) and Notable Labs; SAB: Notable Labs. All other authors have declared no competing interest to disclose.

Received May 6, 2022; accepted in revised form September 23, 2022.

Author Contributions

S.L.S. and C.E.T. conceptualized the project; M.W.R. and S.L.S. were responsible for the methodology; M.W.R. and S.L.S. performed the formal analysis; M.W.R. and S.L.S. investigated; R.J.C., R.D.P., A.F., C.R., G.E., A.R.S., B.W., S.K.M. and J.W.T. provided resources; M.W.R., S.L.S. and C.E.T. wrote the original draft; C.E.T., M.W.R., S.L.S., R.J.C., A.R.S., C.A.E., J.W.T., and B.J.D. reviewed the writing and edited; M.W.R. and S.L.S. visualized the project; C.E.T. supervised; and M.W.R., C.E.T., and B.J.D. acquired funding.

Funding

M.W.R. was supported by the American Society of Hematology (ASH) Physician Scientist Career Development Award. S.L.S. and C.A.E. were supported by an R01 project grant (2R01CA065823-24) to B.J.D. J.W.T. was supported by the V Foundation for Cancer Research, the Gabrielle's Angel Foundation for Cancer Research, the Anna Fuller Fund, the Mark Foundation for Cancer Research, the Silver Family Foundation. Funding for this project was also provided in part by a Leukemia Lymphoma Therapy Acceleration Grant to B.J.D. and J.W.T. and by support provided by the Knight Cancer Research Institute (OHSU). Additional support was provided by grants from the National Cancer Institute (1U01CA217862, 1U54CA224019, 1U01CA214116, 5R01 CA214428-03) and NIH/NCATS CTSA UL1TR002369 (S.K.M. and B.W.).

REFERENCES

Agarwal A, Eide CA, Harlow A, Corbin AS, Mauro MJ, Druker BJ, Corless CL, Heinrich MC, Deininger MW. 2008. An activating *KRAS* mutation in imatinib-resistant chronic myeloid leukemia. *Leukemia* **22:** 2269–2272. doi:10.1038/leu.2008.124

Arber DA, Orazi A, Hasserjian R, Thiele J, Borowitz MJ, Le Beau MM, Bloomfield CD, Cazzola M, Vardiman JW. 2016. The 2016 revision to the World Health Organization classification of myeloid neoplasms and acute leukemia. *Blood* **127:** 2391–2405. doi:10.1182/blood-2016-03-643544

Asmussen J, Lasater EA, Tajon C, Oses-Prieto J, Jun YW, Taylor BS, Burlingame A, Craik CS, Shah NP. 2014. MEK-dependent negative feedback underlies BCR-ABL-mediated oncogene addiction. *Cancer Discov* **4:** 200–215. doi:10.1158/2159-8290.CD-13-0235

Cancer Genome Atlas Research Network, Ley TJ, Miller C, Ding L, Raphael BJ, Mungall AJ, Robertson A, Hoadley K, Triche TJ Jr, Laird PW, et al. 2013. Genomic and epigenomic landscapes of adult de novo acute myeloid leukemia. *N Engl J Med* **368:** 2059–2074. doi:10.1056/NEJMoa1301689

Catalano G, Niscola P, Banella C, Diverio D, Trawinska MM, Fratoni S, Iazzoni R, De Fabritiis P, Abruzzese E, Noguera NI. 2020. NPM1 mutated, BCR-ABL1 positive myeloid neoplasms: review of the literature. *Mediterr J Hematol Infect Dis* **12:** e2020083. doi:10.4084/mjhid.2020.083

Chu S, Holtz M, Gupta M, Bhatia R. 2004. BCR/ABL kinase inhibition by imatinib mesylate enhances MAP kinase activity in chronic myelogenous leukemia $CD34^+$ cells. *Blood* **103:** 3167–3174. doi:10.1182/blood-2003-04-1271

Cibulskis K, Lawrence MS, Carter SL, Sivachenko A, Jaffe D, Sougnez C, Gabriel S, Meyerson M, Lander ES, Getz G. 2013. Sensitive detection of somatic point mutations in impure and heterogeneous cancer samples. *Nat Biotechnol* **31:** 213–219. doi:10.1038/nbt.2514

Conner JR, Smirnova II, Moseman AP, Poltorak A. 2010. IRAK1BP1 inhibits inflammation by promoting nuclear translocation of NF-κB p50. *Proc Natl Acad Sci* **107:** 11477–11482. doi:10.1073/pnas.1006894107

Cuneo A, Ferrant A, Michaux JL, Demuynck H, Boogaerts M, Louwagie A, Doyen C, Stul M, Cassiman JJ, Dal Cin P, et al. 1996. Philadelphia chromosome-positive acute myeloid leukemia: cytoimmunologic and cytogenetic features. *Haematologica* **81:** 423–427.

Deininger MWN, Tyner JW, Solary E. 2017. Turning the tide in myelodysplastic/myeloproliferative neoplasms. *Nat Rev Cancer* **17:** 425–440. doi:10.1038/nrc.2017.40

Döhner H, Wei AH, Roboz GJ, Montesinos P, Thol FR, Ravandi F, Dombret H, Porkka K, Sandhu I, Skikne BS, et al. 2022. Diagnosis and management of AML in adults: 2022 ELN recommendations from an international expert panel. *Blood* **140:** 1345–1377. doi:10.1182/blood.2022016867

Faderl S, Talpaz M, Kantarjian HM, Estrov Z. 1999. Should polymerase chain reaction analysis to detect minimal residual disease in patients with chronic myelogenous leukemia be used in clinical decision making? *Blood* **93:** 2755–2759. doi:10.1182/blood.V93.9.2755

Haferlach T, Nagata Y, Grossmann V, Okuno Y, Bacher U, Nagae G, Schnittger S, Sanada M, Kon A, Alpermann T, et al. 2014. Landscape of genetic lesions in 944 patients with myelodysplastic syndromes. *Leukemia* **28:** 241–247. doi:10.1038/leu.2013.336

Hosseini MM, Kurtz SE, Abdelhamed S, Mahmood S, Davare MA, Kaempf A, Elferich J, McDermott JE, Liu T, Payne SH, et al. 2018. Inhibition of interleukin-1 receptor-associated kinase-1 is a therapeutic strategy for acute myeloid leukemia subtypes. *Leukemia* **32:** 2374–2387. doi:10.1038/s41375-018-0112-2

Hunger SP, Mullighan CG. 2015. Redefining ALL classification: toward detecting high-risk ALL and implementing precision medicine. *Blood* **125:** 3977–3987. doi:10.1182/blood-2015-02-580043

Huntley MA, Larson JL, Chaivorapol C, Becker G, Lawrence M, Hackney JA, Kaminker JS. 2013. ReportingTools: an automated result processing and presentation toolkit for high-throughput genomic analyses. *Bioinformatics* **29:** 3220–3221. doi:10.1093/bioinformatics/btt551

Ilaria RL Jr. 2005. Pathobiology of lymphoid and myeloid blast crisis and management issues. *Hematology Am Soc Hematol Educ Program* **2005:** 188–194. doi:10.1182/asheducation-2005.1.188

Katsumura KR, Mehta C, Hewitt KJ, Soukup AA, de Andrade I F, Ranheim EA, Johnson KD, Bresnick EH. 2018. Human leukemia mutations corrupt but do not abrogate GATA-2 function. *Proc Natl Acad Sci* **115:** E10109–E10118. doi:10.1073/pnas.1813015115

Keung YK, Beaty M, Powell BL, Molnar I, Buss D, Pettenati M. 2004. Philadelphia chromosome positive myelodysplastic syndrome and acute myeloid leukemia-retrospective study and review of literature. *Leuk Res* **28:** 579–586. doi:10.1016/j.leukres.2003.10.027

Koboldt DC, Zhang Q, Larson DE, Shen D, McLellan MD, Lin L, Miller CA, Mardis ER, Ding L, Wilson RK. 2012. VarScan 2: somatic mutation and copy number alteration discovery in cancer by exome sequencing. *Genome Res* **22:** 568–576. doi:10.1101/gr.129684.111

Komorowski L, Fidyt K, Patkowska E, Firczuk M. 2020. Philadelphia chromosome-positive leukemia in the lymphoid lineage-similarities and differences with the myeloid lineage and specific vulnerabilities. *Int J Mol Sci* **21:** 5776. doi:10.3390/ijms21165776

Kurzrock R, Gutterman JU, Talpaz M. 1988. The molecular genetics of Philadelphia chromosome–positive leukemias. *N Engl J Med* **319:** 990–998. doi:10.1056/NEJM198810133191506

Lek M, Karczewski KJ, Minikel EV, Samocha KE, Banks E, Fennell T, O'Donnell-Luria AH, Ware JS, Hill AJ, Cummings BB, et al. 2016. Analysis of protein-coding genetic variation in 60,706 humans. *Nature* **536:** 285–291. doi:10.1038/nature19057

Li H, Durbin R. 2009. Fast and accurate short read alignment with Burrows–Wheeler transform. *Bioinformatics* **25:** 1754–1760. doi:10.1093/bioinformatics/btp324

Liao Y, Smyth GK, Shi W. 2013. The Subread aligner: fast, accurate and scalable read mapping by seed-and-vote. *Nucl Acids Res* **41:** e108. doi:10.1093/nar/gkt214

Liao Y, Smyth GK, Shi W. 2014. featureCounts: an efficient general purpose program for assigning sequence reads to genomic features. *Bioinformatics* **30:** 923–930. doi:10.1093/bioinformatics/btt656

McCarron SL, Maher K, Kelly J, Ryan MF, Langabeer SE. 2013. Rapid evolution to blast crisis associated with a Q252H *ABL1* kinase domain mutation in e19a2 *BCR-ABL1* chronic myeloid leukaemia. *Case Rep Hematol* **2013:** 490740.

McCarthy DJ, Chen Y, Smyth GK. 2012. Differential expression analysis of multifactor RNA-Seq experiments with respect to biological variation. *Nucl Acids Res* **40:** 4288–4297. doi:10.1093/nar/gks042

McKenna A, Hanna M, Banks E, Sivachenko A, Cibulskis K, Kernytsky A, Garimella K, Altshuler D, Gabriel S, Daly M, et al. 2010. The Genome Analysis Toolkit: a MapReduce framework for analyzing next-generation DNA sequencing data. *Genome Res* **20:** 1297–1303. doi:10.1101/gr.107524.110

McLaren W, Pritchard B, Rios D, Chen Y, Flicek P, Cunningham F. 2010. Deriving the consequences of genomic variants with the ensembl API and SNP effect predictor. *Bioinformatics* **26:** 2069–2070. doi:10.1093/bioinformatics/btq330

Nakamura J, Aoyagi S, Nanchi I, Nakatsuka S, Hirata E, Shibata S, Fukuda M, Yamamoto Y, Fukuda I, Tatsumi N, et al. 2009. Overexpression of eukaryotic elongation factor eEF2 in gastrointestinal cancers and its involvement in G2/M progression in the cell cycle. *Int J Oncol* **34:** 1181–1189.

Neuendorff NR, Burmeister T, Dörken B, Westermann J. 2016. BCR-ABL-positive acute myeloid leukemia: a new entity? Analysis of clinical and molecular features. *Ann Hematol* **95:** 1211–1221. doi:10.1007/s00277-016-2721-z

O'Hare T, Walters DK, Stoffregen EP, Jia T, Manley PW, Mestan J, Cowan-Jacob SW, Lee FY, Heinrich MC, Deininger MW, et al. 2005. In vitro activity of Bcr-Abl inhibitors AMN107 and BMS-354825 against clinically relevant imatinib-resistant Abl kinase domain mutants. *Cancer Res* **65:** 4500–4505. doi:10.1158/0008-5472.CAN-05-0259

Oji Y, Tatsumi N, Fukuda M, Nakatsuka S, Aoyagi S, Hirata E, Nanchi I, Fujiki F, Nakajima H, Yamamoto Y, et al. 2014. The translation elongation factor eEF2 is a novel tumor associated antigen overexpressed in various types of cancers. *Int J Oncol* **44:** 1461–1469. doi:10.3892/ijo.2014.2318

Onozawa M, Fukuhara T, Takahata M, Yamamoto Y, Miyake T, Maekawa I. 2003. A case of myelodysplastic syndrome developed blastic crisis of chronic myelogenous leukemia with acquisition of major *BCR/ABL*. *Ann Hematol* **82:** 593–595. doi:10.1007/s00277-003-0703-4

Packer LM, Rana S, Hayward R, O'Hare T, Eide CA, Rebocho A, Heidorn S, Zabriskie MS, Niculescu-Duvaz I, Druker BJ, et al. 2011. Nilotinib and MEK inhibitors induce synthetic lethality through paradoxical activation of RAF in drug-resistant chronic myeloid leukemia. *Cancer Cell* **20:** 715–727. doi:10.1016/j.ccr.2011.11.004

Paietta E, Racevskis J, Bennett JM, Neuberg D, Cassileth PA, Rowe JM, Wiernik PH. 1998. Biologic heterogeneity in Philadelphia chromosome-positive acute leukemia with myeloid morphology: the Eastern Cooperative Oncology Group experience. *Leukemia* **12:** 1881–1885. doi:10.1038/sj.leu.2401229

Patel JP, Gonen M, Figueroa ME, Fernandez H, Sun Z, Racevskis J, Van Vlierberghe P, Dolgalev I, Thomas S, Aminova O, et al. 2012. Prognostic relevance of integrated genetic profiling in acute myeloid leukemia. *N Engl J Med* **366:** 1079–1089. doi:10.1056/NEJMoa1112304

Piedimonte M, Ottone T, Alfonso V, Ferrari A, Conte E, Divona M, Bianchi MP, Ricciardi MR, Mirabilii S, Licchetta R, et al. 2019. A rare *BCR-ABL1* transcript in Philadelphia-positive acute myeloid leukemia: case report and literature review. *BMC Cancer* **19:** 50. doi:10.1186/s12885-019-5265-5

Reboursiere E, Chantepie S, Gac AC, Reman O. 2015. Rare but authentic Philadelphia-positive acute myeloblastic leukemia: two case reports and a literature review of characteristics, treatment and outcome. *Hematol Oncol Stem Cell Ther* **8:** 28–33. doi:10.1016/j.hemonc.2014.09.002

Schlieben S, Borkhardt A, Reinisch I, Ritterbach J, Janssen JW, Ratei R, Schrappe M, Repp R, Zimmermann M, Kabisch H, et al. 1996. Incidence and clinical outcome of children with BCR/ABL-positive acute lymphoblastic leukemia (ALL). A prospective RT-PCR study based on 673 patients enrolled in the German pediatric multicenter therapy trials ALL-BFM-90 and CoALL-05-92. *Leukemia* **10:** 957–963.

Score J, Calasanz MJ, Ottman O, Pane F, Yeh RF, Sobrinho-Simões MA, Kreil S, Ward D, Hidalgo-Curtis C, Melo JV, et al. 2010. Analysis of genomic breakpoints in p190 and p210 BCR-ABL indicate distinct mechanisms of formation. *Leukemia* **24:** 1742–1750. doi:10.1038/leu.2010.174

Soupir CP, Vergilio JA, Dal Cin P, Muzikansky A, Kantarjian H, Jones D, Hasserjian RP. 2007. Philadelphia chromosome–positive acute myeloid leukemia: a rare aggressive leukemia with clinicopathologic features distinct from chronic myeloid leukemia in myeloid blast crisis. *Am J Clin Pathol* **127:** 642–650. doi:10.1309/B4NVER1AJJ84CTUU

Sportoletti P. 2011. How does the *NPM1* mutant induce leukemia? *Pediatr Rep* **3:** e6. doi:10.4081/pr.2011.s2.e6

Tien HF, Wang CH, Chuang SM, Lee FY, Liu MC, Chen YC, Shen MC, Lin DT, Lin KH, Lin KS, et al. 1992. Characterization of Philadelphia-chromosome-positive acute leukemia by clinical, immunocytochemical, and gene analysis. *Leukemia* **6:** 907–914.

Tyner JW, Yang WF, Bankhead A, Fan G, Fletcher LB, Bryant J, Glover JM, Chang BH, Spurgeon SE, Fleming WH, et al. 2013. Kinase pathway dependence in primary human leukemias determined by rapid inhibitor screening. *Cancer Res* **73:** 285–296. doi:10.1158/0008-5472.CAN-12-1906

Tyner JW, Tognon CE, Bottomly D, Wilmot B, Kurtz SE, Savage SL, Long N, Schultz AR, Traer E, Abel M, et al. 2018. Functional genomic landscape of acute myeloid leukaemia. *Nature* **562:** 526–531. doi:10.1038/s41586-018-0623-z

Zhang H, Wilmot B, Bottomly D, Dao KT, Stevens E, Eide CA, Khanna V, Rofelty A, Savage S, Reister Schultz A, et al. 2019. Genomic landscape of neutrophilic leukemias of ambiguous diagnosis. *Blood* **134:** 867–879. doi:10.1182/blood.2019000611